Einstein crystal as a reference system in free energy estimation using adiabatic switching

M. de Koning and A. Antonelli
Instituto de Física Gleb Wataghin, Universidade Estadual de Campinas, Unicamp 13083-970, Campinas, São Paulo, Brazil
(Received 2 August 1995)

In this paper we investigate the behavior of an Einstein crystal as a reference system in adiabatic switching procedures. We study the canonical massive Nosé-Hoover chain (MNHC) dynamics [G.J. Martyna, M.L. Klein, and M. Tuckerman, J. Chem. Phys. **97**, 2635 (1992)] and show it can be used to determine Helmholtz free energies within an adiabatic switching procedure. We calculate the Helmoltz free energy difference between two different Einstein crystals, each consisting of 100 identical independent harmonic oscillators with different characteristic frequencies by a MNHC molecular dynamics adiabatic switching procedure. The simulations were performed using two different switching functions. Applying the quantitative error analysis of Tsao, Sheu, and Mou [J. Chem. Phys. **101**, 2302 (1994)], it is found that systematic errors during the switching process can be estimated quantitatively, allowing a correction of the converged results. The corrected results obtained by adiabatic switching deviate less than 1% from the analytical value. It is observed that quantitative correction of converged results can be avoided by choosing a proper switching function.

PACS number(s): 05.70.−a, 02.70.−c, 63.70.+h, 65.50.+m

I. INTRODUCTION

Molecular dynamics (MD) is a simulation technique widely used in the statistical treatment of classical many-body systems [1–3]. One of the principal applications of MD concerns determination of thermodynamic properties of liquids and solids. The determination of free energies is of considerable interest, from both the scientific and technological points of view, since they play a crucial role in several physical phenomena such as phase transitions and vacancy formation processes. The main problem in determining thermal quantities using MD is the fact that they are functions of the total available phase-space volume. Consequently, they cannot be expressed as an ensemble average, which is possible for properties such as internal energy, enthalpy, and temperature, which are explicit functions of the phase-space coordinates.

In the literature, several computational methods based on different philosophies have been used to determine free energies using MD simulations. The quasiharmonic (QH) [5–7] and local harmonic (LH) [4,6] methods are based on the so-called harmonic approximation. This approximation assumes that, when the deviations of the atoms from their equilibrium positions are small, the lattice energy U can be approximated by expansion about its equilibrium value, including terms up to second order in the atomic deviations. In this case, the system is completely described by the dynamical matrix $\mathbf{D}$ and the Helmholtz free energy is determined in terms of its eigenfrequencies. The main disadvantage of the QH and LH methods, aside from the computationally demanding diagonalization procedures, is the fact that the approximations involved generally lose validity under conditions near phase transitions.

An alternative method, which in principle is exact, is the thermodynamic integration (TI) procedure [8]. This procedure determines the free energy difference ΔF between the system of interest described by a Hamiltonian H_0 and a certain reference system described by H_1. Introducing the coupling parameter λ, which varies between 0 and 1, a composite Hamiltonian

$$H = \lambda H_0 + (1-\lambda)H_1 = K + \lambda U + (1-\lambda)V, \quad (1.1)$$

where K represents the kinetic energy, U the potential energy of the system of interest, and V the potential energy of the reference system, is constructed. The Helmholtz free energy difference between the systems of interest and reference is then given by

$$\Delta F = \int_0^1 \left\langle \frac{\partial H}{\partial \lambda} \right\rangle_\lambda d\lambda = \int_0^1 \langle U - V \rangle_\lambda \, d\lambda. \quad (1.2)$$

The numerical evaluation of the integral in Eq. (1.2) requires a set of equilibrium MD simulations based on the composite Hamiltonian (1.1) for various fixed values of λ between 0 and 1. During every simulation, the equilibrium ensemble average $\langle U - V \rangle_\lambda$ corresponding to a certain value of λ is determined after which a numerical estimate of the integral can be made. Although exact, the TI method is computationally rather demanding since several runs have to be executed, each of them requiring sufficient equilibration and sampling time.

In 1990, Watanabe and Reinhardt [9] proposed the adiabatic switching method, which is based on the Hertz ergodic invariance principle [10]. This principle states that, in an adiabatic transformation of a system described by an ergodic, deterministic, Hamiltonian energy conserving dynamics D_0 into another system described by D_1, a constant energy shell $\sigma(E_0, D_0)$ with phase volume Ω is precisely mapped upon the constant energy shell $\sigma(E_1, D_1)$ which has exactly the same phase-space volume Ω. The

original demonstration of the principle by Hertz has been included in the Appendix and it has to be emphasized that the derivation does not explicitly require the dynamics to be Hamiltonian. However, as we will see later, the use of the Hertz principle within a non-Hamiltonian dynamics may involve certain technical problems which compromise the rigorous theoretical basis of its application. The simplest application of Hertz's principle is an adiabatic transformation between two ergodic Hamiltonian systems. In this case, a time dependent Hamiltonian

$$H(t) = \lambda(t)H_0 + [1 - \lambda(t)]H_1 \tag{1.3}$$

is introduced. H_0 describes the system of interest and H_1 represents some system of reference. The coupling parameter λ changes slowly and smoothly from 1 to 0, establishing the slow switching from H_0 to H_1. If the switching is adiabatic and both H_0 and H_1 are ergodic, a classical trajectory governed by (1.3) connects a constant energy shell $\sigma(E_0)$ of H_0 with unknown entropy with a constant energy shell $\sigma(E_1)$ of H_1 with the same entropy. Now, if we know the corresponding entropy $S_{ref}(E_1)$ of the reference system, we automatically know that for the system of interest this entropy corresponds with the energy E_0. Thus, in principle, the computation of a single classical trajectory based on (1.3) is sufficient to determine the entropy S_{syst} corresponding with energy E_0.

Besides this application, Watanabe and Reinhardt showed that the adiabatic invariant is also useful using a dynamics other than the standard Hamiltonian dynamics. They showed, for instance, [9] that if the adiabatic switching procedure is performed under the extended Hamiltonian (constant temperature) Nosé dynamics [11,12], the Helmholtz free energy difference between the system of interest and reference at temperature T can be determined directly from a single trajectory and is given by the difference between the initial and final energies of the extended Nosé Hamiltonian in the switching process.

Adiabatic switching is a flexible and computationally relatively inexpensive method. It does not rely on any approximation and the needed information can, in principle, be determined from a single trajectory. In this sense, adiabatic switching does not present the disadvantages inherent in the harmonic and thermodynamic integration methods.

Despite the computationally promising features, application of adiabatic switching in a realistic simulation situation presents some difficulties which inhibit the validity of the Hertz invariance principle. First, there is the question of ergodicity. Strictly speaking, ergodicity of the dynamics at any stage during the switching process is a necessary condition for the validity of the Hertz invariance theorem. However, in their simulations computing the entropy of liquid water using adiabatic switching, Watanabe and Reinhardt observed convergence of the final energy of the switching process for switching times very short compared to the ergodic time scale. Apparently, ergodicity does not seem to be such a critical condition. A more important problem is the fact that in simulations only finite (nonadiabatic) switching rates can be used. As a result, one cannot rely on pointwise mapping of constant energy shells in a realistic simulation situation.

In 1992, Jarzynski [13] presented a mathematical analysis studying the effects of finite switching rates on the conservation of the adiabatic Hertz invariant. The analysis confirms that for finite switching rates there is no pointwise mapping of an initial constant energy shell onto a final constant energy shell. Instead, Jarzynski showed that the time evolution of the energy distribution function is governed by a diffusion equation. Based on this equation, he showed that an initial δ energy distribution function diffuses into a final Gaussian energy distribution function of finite width. Furthermore, it was found that the mean of the Gaussian is shifted towards a higher energy relative to the position of the adiabatic final δ energy distribution function.

In this manner, it is clear that in a realistic simulation situation a single trajectory estimate is subject to two kinds of error. First, there is a statistical error due to the finite width of the final distribution. Secondly, there is a systematic error caused by a shift of the mean with respect to the position of the final δ energy distribution of the pointwise mapping process. Determination of the statistical error is relatively easy by calculating a small number of trajectories and estimating the mean and the variance of the final energies. On the other hand, the estimation of the systematic error is rather complicated. The expressions derived by Jarzynski are not convenient to be used in a simulation situation.

Very recently, Tsao, Sheu, and Mou [14] presented an alternative analysis of the effects of finite switching rates on adiabatic switching. In their analysis, which is based on a thermodynamic rather than a mathematical approach, they derive an expression for the growth of the systematic error during the switching process. The advantage of this expression over the one derived by Jarzynski is the fact that the former is physically more transparent which allows an easier application in realistic switching processes. In their paper, Tsao *et al.* apply the adiabatic switching method to calculate the absolute entropy of water and ice. Based on their systematic error expression, they qualitatively show that the choice of the combination of reference system and switching function has a decisive influence on the goodness of the results of adiabatic switching.

In this paper, it is our objective to study an Einstein crystal in canonical ensemble adiabatic switching processes. The Einstein crystal is of considerable interest since it is the most suitable reference system in adiabatic switching processes involving real solids. It is particularly interesting to see how such processes behave under constant temperature conditions since, in principle, they allow determination of the Helmholtz free energies of realistic solids. For this purpose, we applied the adiabatic switching method to determine the Helmholtz free energy of an Einstein crystal consisting of 100 identical independent harmonic oscillators. As a reference, we used another Einstein crystal having the same configurational structure but a different characteristic frequency. The

switching simulations were performed using the canonical massive Nosé-Hoover chain (MNHC) dynamics introduced by Martyna, Klein, and Tuckerman [15], which has been shown to generate the canonical distribution for a system of independent harmonic oscillators [16]. This dynamics is a modification of the original Nosé-Hoover chain (NHC) dynamics, which has been used recently by Holian, Posch, and Hoover [17] to compute the Helmholtz free energy of a six-body harmonic chain by dynamic TI methods. Finally, we apply the error analysis of Tsao *et al.* to study the goodness of the obtained results in a quantitative manner.

In Sec. II, we give a summary of the results of the error analysis of adiabatic switching as presented by Tsao *et al.* and discuss means by which their analysis can be applied in a quantitative manner. In Sec. III, we focus on the dynamics of the MNHC method and discuss its application in an adiabatic switching procedure. We show that the derivation of Watanabe and Reinhardt regarding Helmholtz free energy determination by adiabatic switching procedures using the Nosé dynamics presents formal problems when applied to switching processes within the non-Hamiltonian MNHC dynamics. Instead, we use a thermodynamic argument to explain that the Helmholtz free energy determination should be the same in both cases. In Sec. IV, we first describe the computational details of the simulations, after which we present and discuss the obtained results. We end with conclusions in Sec. V.

II. ERROR ANALYSIS

We consider an adiabatic switching process transforming a system described by the dynamics D_0 (not necessarily Hamiltonian) into another system D_1. D_0 conserves the Hamiltonian energy $E = K + U$ whereas D_1 conserves $E = K + V$. The switching process is controlled by the time dependent coupling parameter $\lambda(t)$ which decreases from 1 to 0 in a total switching time t_s. The instantaneous dynamics $D(\lambda)$ determined by λ conserves $E = K + \lambda U + (1 - \lambda)V$. Obviously, $D(1) = D_0$ and $D(0) = D_1$.

If the switching is adiabatic (infinite t_s), the Hertz invariance principle guarantees that a constant energy shell $\sigma(K + U, D_0)$ is mapped upon the constant energy shell $\sigma(K + V, D_1)$ having the same phase-space volume Ω. In the case of finite (nonadiabatic) switching times, an initial δ function energy distribution diffuses into a Gaussian distribution of finite width. The difference between adiabatic and nonadiabatic switching has been depicted schematically in Fig. 1. In addition to the stochastic broadening M_2, the mean of the Gaussian is shifted by an amount M_1 with respect to the position of the adiabatic δ function energy distribution. This systematic shift M_1 is caused by dissipative relaxation of the particle configurations near to equilibrium towards equilibrium. In a perfectly adiabatic process, the switching rate is infinitely slow so that the configurations remain representative for the instantaneous dynamics (i.e., in equilibrium) at all times. However, if the switching rate $d\lambda/dt$ is

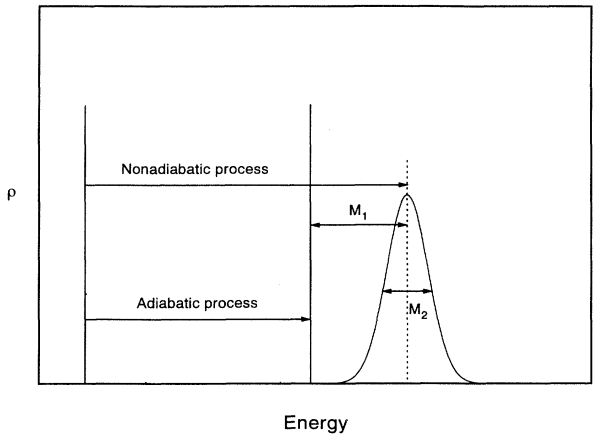

FIG. 1. Evolution of initial δ function energy distribution due to adiabatic and nonadiabatic switching.

finite, finite changes in the instantaneous dynamics occur at any instant during the switching, making the process typically nonequilibrium. The relaxation of the particle configurations may be described in terms of a characteristic time lag τ_{lag}. This time lag is regarded as the time the configurations lag the actual dynamics.

Now, although the process is a nonequilibrium one, the configurations remain near equilibrium (because of the, although finite, small switching rates) which enables a linear response analysis of the time lag. We will discuss this point in more detail later in this section.

The width M_2 reflects the chaotic nature of the trajectory dynamics. Different trajectories with the same initial energy will generally pass through different near-to-equilibrium states. As a consequence, different trajectories are subject to different time lags during the switching, which leads to the diffusive broadening.

Tsao *et al.* have derived an expression for dM_1/dt in terms of the switching rate $d\lambda/dt$ and the time lag τ_{lag}. Regarding the system described by (1.3) as a linear nonequilibrium thermodynamic system they find that dM_1/dt is given by

$$\frac{dM_1}{dt} = \frac{1}{kT}\tau_{lag}\left(\frac{d\lambda}{dt}\right)^2 \mathrm{var}(U - V)_t, \tag{2.1}$$

where k is Boltzmann's constant, T is the absolute temperature, and $\mathrm{var}(U-V)_t$ is the canonical ensemble variance of the phase-space function $U - V$ for the static system described by (1.3) with a specific fixed value of λ corresponding to t. Generally, τ_{lag} and $\mathrm{var}(U - V)_\lambda$ depend on λ (and thus on time in the switching process). Note that (2.1) is a positive definite expression. In this manner, the average nonadiabatic energy is always larger than the adiabatic energy.

A time integration of (2.1) over the switching time interval gives the total systematic error M_1 of the process;

$$M_1 = \frac{1}{kT}\int_0^{t_s} \tau_{lag}\left(\frac{d\lambda}{dt}\right)^2 \mathrm{var}(U - V)_t dt. \tag{2.2}$$

Introducing the scaled variable $\tau = t/t_s$ (2.2) can be

rewritten as

$$M_1 = \frac{1}{kTt_s}\int_0^1 \tau_{lag}\left(\frac{d\lambda}{d\tau}\right)^2 \mathrm{var}(U-V)_\tau d\tau. \quad (2.3)$$

Tsao *et al.* have shown that (2.1) is of considerable help in the choice of the switching function $\lambda(t)$ and the reference system V. They argued that one should choose the switching rate to be smaller in regions of slow relaxation or large fluctuations in $U-V$. To test their ideas, they applied the adiabatic switching method to compute the absolute entropy of single point charge (SPC) water and ice. Their simulations were performed using standard Hamiltonian dynamics and as reference systems the ideal gas ($V=0$) and the Einstein crystal [$V=\frac{1}{2}\sum_{i=1}^{n}\kappa(x_i-x_{i0})^2$] were investigated. As switching functions, they analyzed the functions

$$\lambda(\tau) = C_1(\tau) = 1-\tau^5(70\tau^4-315\tau^3+540\tau^2-420\tau+126) \quad (2.4)$$

and

$$\lambda(\tau) = C_2(\tau) = (1-\tau)^5. \quad (2.5)$$

Plots of (2.4) and (2.5) can be found in Fig. 2 and we see that both switching functions have a vanishing slope at the end of the switching process. According to Tsao *et al.* this is necessary because the time lag τ_{lag} diverges at the independent particle end of the switching. Their simulations show that the best results of the adiabatic switching method applied for both SPC water and ice are obtained using $C_2(\tau)$ as switching function and the Einstein crystal as a reference. They explain these results by arguing that $\mathrm{var}(U-V)$ using the Einstein solid is smaller than for the ideal gas reference system. Furthermore, $C_2(\tau)$ approaches the independent particle end of the switching process (diverging τ_{lag}) with a smaller rate than $C_1(\tau)$.

From the results of Tsao *et al.* we see that expression (2.1) can be used as a guideline to a suitable choice of switching functions and reference systems in an adiabatic switching procedure. Nevertheless, we should be able to go beyond this and use the integral expression (2.2) to explicitly calculate the systematic error in an adiabatic switching procedure.

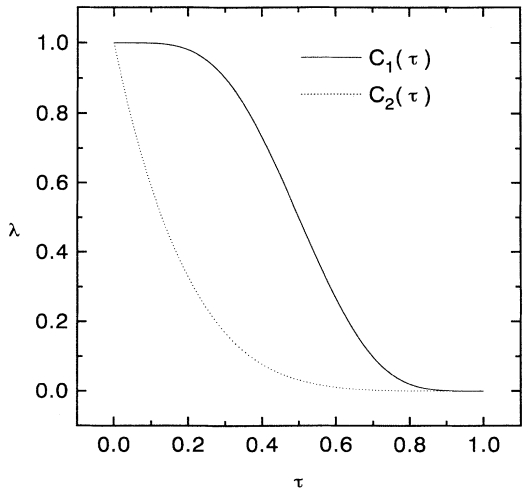

FIG. 2. Switching functions $C_1(\tau)$ and $C_2(\tau)$.

The main problem is to find a suitable way of measuring the time lags τ_{lag}. Recently, Wood [18] used Onsager's principle [19] to achieve this goal. Onsager's principle states that when a system is not too far from equilibrium the relaxation of any mechanical property obeys

$$\frac{\Delta\overline{A}(t)}{\Delta\overline{A}(0)} = \frac{C(t)}{C(0)}, \quad (2.6)$$

where

$$\Delta\overline{A}(t) = \overline{A}(t) - \langle A\rangle_{E_0} = \delta\overline{A}(t) \quad (2.7)$$

and

$$C(t) = \lim_{\tau\to\infty}\frac{1}{\tau}\int_0^\tau d\bar{t}\;\delta A(\bar{t})\;\delta A(\bar{t}+t) \quad (2.8)$$

is the equilibrium time autocorrelation function. Thus in principle we should be able to use the decay time of the equilibrium autocorrelation function of $U-V$ to estimate the time lags.

The other quantity to be determined is $\mathrm{var}(U-V)$. This variance is a canonical ensemble variance which can be easily determined in an equilibrium canonical ensemble simulation.

III. ADIABATIC SWITCHING USING THE MNHC DYNAMICS

In 1984, Nosé [11] proposed a set of dynamical equations that can be shown to generate canonically distributed positions and momenta for ergodic systems. Although Nosé's method has proved to work well for strongly coupled systems, it fails for small or stiff systems. To overcome this problem, several authors have studied alternative methods [20–22]. The most appealing method was proposed recently by Martyna, Klein, and Tuckerman [15]. The dynamics they presented is capable of generating the canonical distribution for a single harmonic oscillator without giving up the simplicity of the original Nosé approach. Their method, which they called the Nosé-Hoover chain (NHC) method, can be expressed as

$$\begin{aligned}
\dot{q}_i &= \frac{p_i}{m_i},\\
\dot{p}_i &= -\frac{\partial V}{\partial q_i} - p_i\frac{p_{\eta_1}}{Q_1},\\
\dot{\eta}_i &= \frac{p_{\eta_i}}{Q_i},\\
\dot{p}_{\eta_1} &= \left[\sum_{i=1}^{n}\frac{p_i^2}{m_i} - nkT\right] - p_{\eta_1}\frac{p_{\eta_2}}{Q_2},\\
\dot{p}_{\eta_j} &= \left[\frac{p_{\eta_{j-1}}^2}{Q_{j-1}} - kT\right] - p_{\eta_j}\frac{p_{\eta_{j+1}}}{Q_{j+1}},\\
\dot{p}_{\eta_M} &= \left[\frac{p_{\eta_{M-1}}^2}{Q_{M-1}} - kT\right],
\end{aligned} \quad (3.1)$$

where the p_i and q_i describe the n one-dimensional degrees of freedom of the physical system, m_i the masses of the physical degrees of freedom, and the η_i and the p_{η_i} represent the coordinates and the momenta of the M external degrees of freedom (thermostats). The parameters Q_i act as moments of inertia for the motion of the thermostats. Furthermore, k is Boltzmann's constant and T is the absolute temperature. Investigating the structure of the set of equations (3.1), it can be seen that the M thermostats form a linear chain of which only the first thermostat η_1 is coupled directly to the physical system. The NHC method generates states $(\vec{p}, \vec{q}, \vec{p}_\eta, \vec{\eta})$ according to the distribution function

$$\rho(\vec{p}, \vec{q}, \vec{p}_\eta, \vec{\eta}) \propto \exp\left\{ -\frac{1}{kT}\left[V(\vec{q}) + \sum_{i=1}^{n} \frac{p_i^2}{2m_i} + \sum_{i=1}^{M} \frac{p_{\eta_i}^2}{2Q_i} \right] \right\} \tag{3.2}$$

and conserves the Hamiltonian-like energy

$$E(\vec{p}, \vec{q}, \vec{p}_\eta, \vec{\eta}) = V(\vec{q}) + \sum_{i=1}^{n} \frac{p_i^2}{2m_i} + \sum_{i=1}^{M} \frac{p_{\eta_i}^2}{2Q_i} + nkT\eta_1 + \sum_{i=2}^{M} kT\eta_i. \tag{3.3}$$

This implies that in the extended phase space (3.1) generates a microcanonical distribution. The moments of inertia Q_i should be chosen to be $Q_1 = nkT/\omega^2$ and $Q_i = kT/\omega^2$ to establish near resonance between the individual thermostats and between the thermostat system and the physical phase-space coordinates (p_i, q_i).

Although the NHC dynamics is capable of generating the canonical distribution for a single harmonic oscillator, it is not for a system of n independent harmonic oscillators, as was shown very recently by Smargiassi and Madden [16]. To solve this problem, the so-called massive Nosé-Hoover chain (MNHC) dynamics can be used. The difference between NHC and MNHC dynamics is that, instead of a single linear chain of M thermostats connected to the physical system, the MNHC dynamics couples n linear chains each consisting of two or more thermostats to the n physical degrees of freedom. The equations of motion of the MNHC method (chains of two thermostats) are

$$\begin{aligned}
\dot{q}_i &= \frac{p_i}{m_i}, \\
\dot{p}_i &= -\frac{\partial V}{\partial q_i} - p_i \frac{p_{\eta_{i,1}}}{Q_i}, \\
\dot{\eta}_{i,1} &= \frac{p_{\eta_{i,1}}}{Q_i}, \\
\dot{\eta}_{i,2} &= \frac{p_{\eta_{i,2}}}{Q_i}, \\
\dot{p}_{\eta_{i,1}} &= \frac{p_i^2}{m_i} - kT - p_{\eta_{i,1}} \frac{p_{\eta_{i,2}}}{Q_i}, \\
\dot{p}_{\eta_{i,2}} &= \frac{p_{\eta_{i,1}}^2}{Q_i} - kT,
\end{aligned} \tag{3.4}$$

which generate the distribution (3.2). In extended phase space (3.4) generates the microcanonical distribution with energy

$$E(\vec{p}, \vec{q}, \vec{p}_\eta, \vec{\eta}) = V(\vec{q}) + \sum_{i=1}^{n} \frac{p_i^2}{2m_i} + \sum_{i=1}^{n} \frac{p_{\eta_{i,1}}^2 + p_{\eta_{i,2}}^2}{2Q_i} + \sum_{i=1}^{n} kT(\eta_{i,1} + \eta_{i,2}). \tag{3.5}$$

In principle, as with the canonical Nosé dynamics, it should be possible to determine Helmholtz free energies by an adiabatic switching procedure using the canonical MNHC dynamics. However, a theoretical demonstration of this is far from straightforward. Watanabe and Reinhardt utilized the partition function of the microcanonical ensemble corresponding to the Nosé dynamics to demonstrate the possibility of determining Helmholtz free energies by an adiabatic switching procedure using the Nosé dynamics. Nosé found this microcanonical partition function to be of the form

$$Z_\mu(E_m) = C \exp\left(\frac{E_m}{kT}\right) Z_c(T), \tag{3.6}$$

where C is a constant and $Z_c(T)$ is the canonical partition function of the physical system at temperature T. For the non-Hamiltonian MNHC dynamics, however, it can be shown that its corresponding microcanonical partition function is singular. This singularity is due to the configurational part of the thermostats in this partition function. Because of the presence of more than one thermostat, the thermostat coordinate subspace $\{\eta_{i,1}, \eta_{i,2}, i = 1, \ldots, N\}$ of any constant energy shell is unbounded (e.g., see Appendix A of Ref. [15]) which leads to an infinite phase-space volume. In the case of the Nosé dynamics this problem does not occur since only one thermostat is included so that its corresponding subspace is bounded. It is not clear to us to what extent the singularity in the microcanonical partition function is related to the fact of the MNHC dynamics being non-Hamiltonian.

Instead of relying on a statistical-mechanical analysis, which reflects specific details of the dynamics used, we feel it is very illuminating to consider adiabatic switching processes within canonical ensemble dynamics from the thermodynamic point of view. The advantage of such an approach is that we do not need to consider any specific details of the switching procedure or the dynamics used but rather concentrate on the macroscopic thermodynamic system they represent. In this case, we consider a system A composed of a system of interest A_1 which is in thermal equilibrium with a heat reservoir A_2 at temperature T. In principle, A is closed so that the total internal energy remains constant. Then, at a certain instant we open the system and invoke an external work source which performs reversible work on the system of interest A_1 at an adiabatic rate without exchanging any heat. How do the internal energies (E_1, E_2), entropies (S_1, S_2), and Helmholtz free energies (F_1, F_2) of A_1 and A_2 change during this adiabatic isothermal process? Let us consider the change of these quantities due to an in-

finitesimal amount of work dW done on A_1. According to the first law of thermodynamics we have

$$dE_1 = TdS_1 + dW, \tag{3.7}$$

$$dE_2 = TdS_2, \tag{3.8}$$

observing that the heat reservoir cannot perform any work. Furthermore, since the process is adiabatic, the total entropy change satisfies

$$dS = dS_1 + dS_2 = 0. \tag{3.9}$$

The changes in the Helmholtz free energies of the subsystems A_1 and A_2 are

$$dF_1 = dE_1 - TdS_1, \tag{3.10}$$

$$dF_2 = dE_2 - TdS_2. \tag{3.11}$$

Adding (3.10) and (3.11) we obtain

$$dF_1 + dF_2 = dE_1 + dE_2 - T(dS_1 + dS_2). \tag{3.12}$$

The Helmholtz free energy change of the heat reservoir satisfies $dF_2 = 0$ as can be seen from (3.8) and (3.11). Inserting this information and (3.9) into (3.12) we obtain

$$dF_1 = dE_1 + dE_2. \tag{3.13}$$

Thus we see that the change of the Helmholtz free energy of subsystem A_1 is equal to the change of the total internal energy of the composite system A. For the complete process, the total Helmholtz free energy change of the physical system will be

$$\Delta F_1 = \Delta E_1 + \Delta E_2. \tag{3.14}$$

This is exactly the same result as derived by Watanabe and Reinhardt for adiabatic switching procedures using Nosé dynamics. This agreement seems reasonable since the dynamics of these procedures contains all microscopic elements necessary to fulfill the macroscopic thermodynamic conditions of the analysis above. First of all, the thermostat subsystem of the Nosé dynamics maintains the physical system and itself at a constant temperature. This is accomplished exclusively by exchanging heat. The thermostat system cannot perform any work since no external parameters are present in its equations of motion. Secondly, the Nosé dynamics conserves the total energy of the extended system representing the condition that the extended system is closed. Finally, the adiabatic reversible work done by the external source is represented by the coupling parameter λ which varies very slowly in time. Clearly, the external work is done without any heat exchange since the only link between the physical system and the work source is the parameter λ. Thus we see that the microscopic properties of adiabatic switching procedures using Nosé dynamics are compatible with the macroscopic conditions of the thermodynamic adiabatic isothermal process described earlier.

If we have a look at adiabatic switching processes using the MNHC dynamics, we see that, although quite different from those of the Nosé dynamics, the equations of motion are compatible with the same macroscopic conditions. Therefore, adiabatic switching procedures using the MNHC dynamics represent adiabatic isothermal processes in the thermodynamic sense and thus we expect that they can be used to determine Helmholtz free energies by applying (3.14).

IV. CALCULATIONS AND RESULTS

In this section we describe the computational details and the results of the calculations performed to test the error analysis of Tsao *et al.* and investigate the possibility of using an Einstein crystal as a reference system during a constant temperature switching procedure within MNHC dynamics. In the adiabatic switching simulations, the system of interest was an Einstein crystal consisting of 100 identical independent one-dimensional harmonic oscillators with $m = 1$ and $\omega = 0.5$. As the system of reference we used another Einstein crystal having the same structure, equal masses, but a different characteristic angular frequency $\omega = 4$. The adiabatic switching procedures were performed within the MNHC dynamics (3.4) with $kT = 1$. For the value of $Q = kT/\omega^2$ we took $Q = 0.25$ which corresponds with the intermediate frequency $\omega = 2$. We checked that the dynamics using this value of Q generated canonically distributed momenta during the switching. The equations of motion of the MNHC dynamics were integrated using the leapfrog algorithm [23] with a time step $\Delta t = 0.01$. As switching functions both (2.4) and (2.5) were investigated.

In Fig. 3 we plotted the Helmholtz free energy differ-

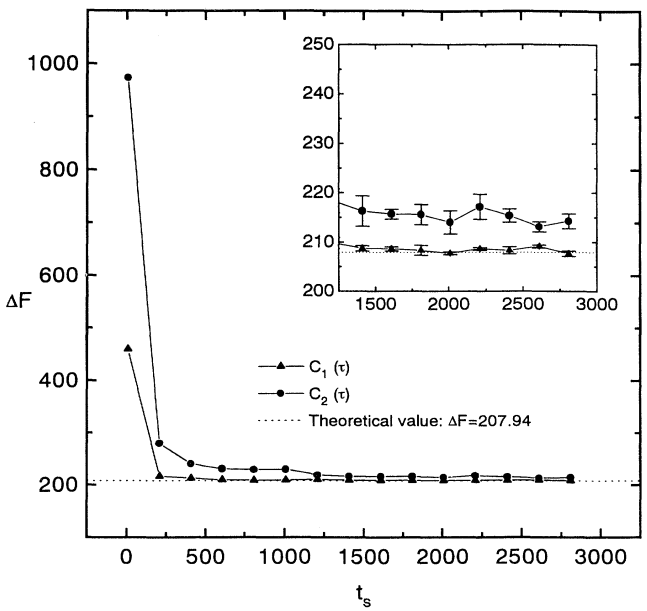

FIG. 3. Helmholtz free energy difference between two Einstein crystals consisting of 100 identical independent harmonic oscillators as a function of t_s. Initial crystal, $m = 1, \omega = 0.5$; final crystal, $m = 1, \omega = 4$. During the switching we set $kT = 1$. Results are displayed for both $C_1(\tau)$ and $C_2(\tau)$.

ence (3.14) between the systems of interest and reference as a function of the switching time t_s for both $C_1(\tau)$ and $C_2(\tau)$. The statistical errors associated with each t_s were estimated by computing five trajectories with different initial conditions.

The switching procedure using $C_1(\tau)$ converges faster than the switching with $C_2(\tau)$. Furthermore, we observe that the converged free energy difference using $C_1(\tau)$ agrees very well with the theoretical value within the statistical error. This confirms the applicability of adiabatic switching using the MNHC dynamics to determine Helmholtz free energies. On the other hand, the converged estimate using $C_2(\tau)$ is systematically higher. The statistical errors decrease with increasing switching time and for $C_1(\tau)$ they are smaller than for $C_2(\tau)$.

To correct the final estimates of the switching procedure, we calculated the systematic errors based on (2.3). For these purposes, several equilibrium constant temperature simulations were performed at various fixed values of the coupling parameter λ. From these simulations, we estimated the variances $\mathrm{var}(U-V)$ as a function of λ. Furthermore, we calculated the autocorrelation functions $C_{U-V}(\tau)$ to estimate the time lags τ_{lag}. In Fig. 4 we plotted the autocorrelation function for $\lambda = 0.7$. We defined the time lag to be the time corresponding with the first intersection with the τ axis.

In Fig. 5 and Fig. 6, respectively, we plotted $\mathrm{var}(U-V)$ and τ_{lag} as a function of λ. In Fig. 5 we added the analytical expression for $\mathrm{var}(U-V)$ to check the reliability of the numerical results. The analytical expression is given by

$$\mathrm{var}(U-V)_\lambda = \frac{1}{2}Nk^2T^2\left(\frac{\omega_1^2-\omega_2^2}{\lambda\omega_1^2+(1-\lambda)\omega_2^2}\right)^2, \quad (4.1)$$

where ω_1 and ω_2 are, respectively, the initial and final frequencies of the switching process. The agreement between the exact values and the numerical results is excellent.

We observe that in the initial stages of the switching

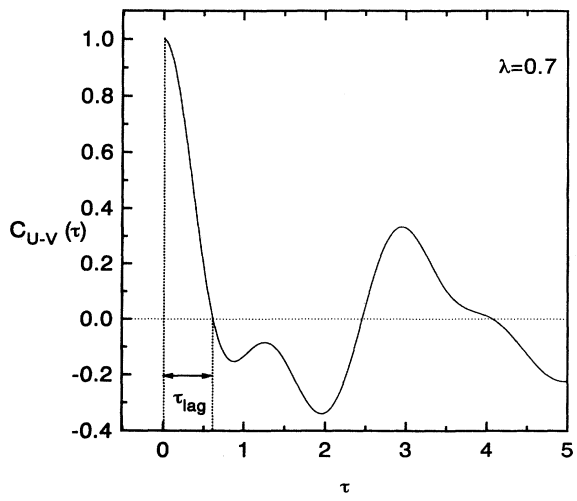

FIG. 4. Autocorrelation function $C_{U-V}(\tau)$ for $\lambda = 0.7$.

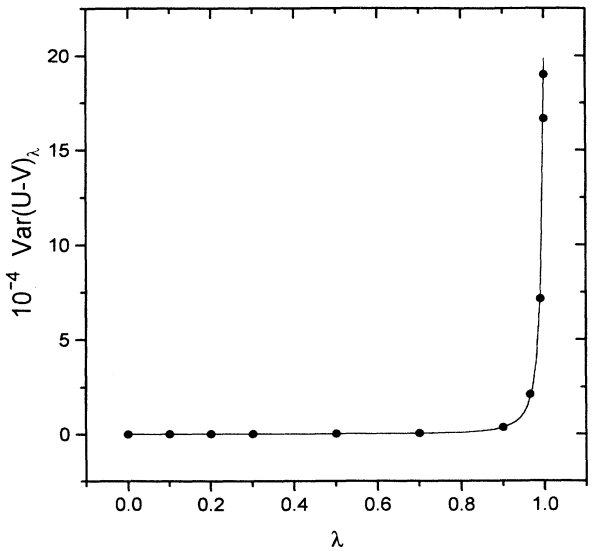

FIG. 5. $\mathrm{var}(U-V)$ as a function of λ. The circles represent the numerical data; the line represents the exact values of expression (4.1).

(λ near to 1) the variance is the dominant factor in the error function. Therefore one should choose a switching function with a vanishing slope in the beginning of the switching. Based on the data in Fig. 5 and Fig. 6 we constructed the integrand in (2.3) as a function of τ for both switching functions. The results have been depicted in Fig. 7 and Fig. 8.

Because of its vanishing slope in the beginning, $C_1(\tau)$ manages to control the integrand whereas $C_2(\tau)$ cannot prevent the near singularity for $\tau = 0$. We integrated both error functions between $\tau = 0$ and $\tau = 1$ to find estimates for the systematic error of the switching process with $t_s = 2800$. In Table I we have summarized the

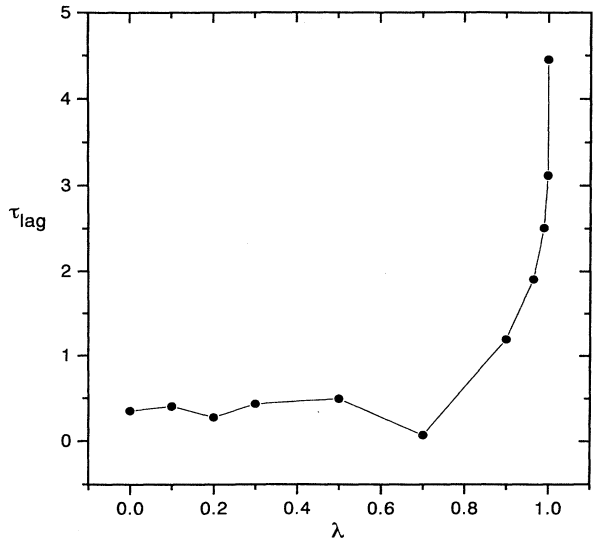

FIG. 6. Time lag τ_{lag} as a function of λ.

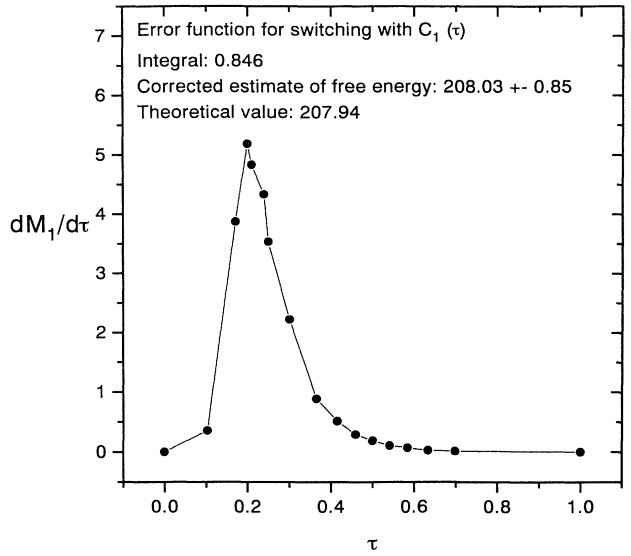

FIG. 7. Error function for $C_1(\tau)$.

results. In the second column we placed the converged results of the switching procedures, in the third the statistical errors, in the fourth the systematic errors, and in the last the final result in which a correction for the systematic errors has been taken into account.

From Table I we see that both corrected results deviate by less than 0.5% from the theoretical result, which is a surprisingly good agreement and it confirms the quantitative applicability of the error analysis of Tsao *et al.* If we consider the uncorrected results in the second column we observe that, choosing the better switching function $C_1(\tau)$, we manage to keep the error (systematic and statistical) within 1%.

Finally we feel it is important to emphasize that one cannot speak of globally "good" or "bad" switching functions. The goodness of a switching function differs for every specific switching process and this has to be evaluated for each separate case. To improve the quantitative results of the method one should always choose the reference system "as close as possible" to the system of interest. For example, if we use an Einstein crystal as a reference system in an adiabatic switching process involving a real solid, we should choose its frequencies according to the principal vibrational modes of the real solid.

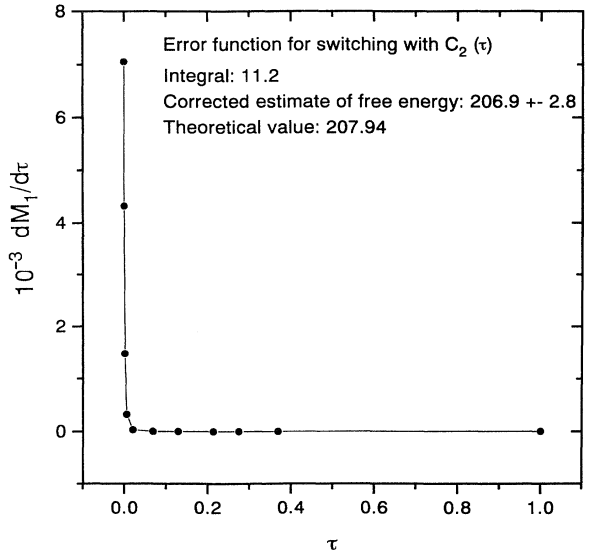

FIG. 8. Error function for $C_2(\tau)$.

TABLE I. Results of adiabatic switching simulations. In the second column the uncorrected estimates of ΔF are depicted. In the third and fourth columns respectively, the systematic and statistical errors are shown. In the fifth column, we show the estimates corrected for the systematic errors.

$\lambda(\tau)$	ΔF	M_1	M_2	Corrected ΔF
$C_1(\tau)$	208.88	0.85	0.85	208.03 ± 0.85
$C_2(\tau)$	218.1	11.2	2.8	206.9 ± 2.8

V. CONCLUSIONS

The results of the last section confirm that adiabatic switching procedures using MNHC dynamics allow determination of Helmholtz free energies. The simulations show that it is possible to use the Einstein crystal as a reference system in an adiabatic switching procedure within constant temperature MNHC dynamics. This allows application of the adiabatic switching method to determine Helmholtz free energies of realistic solids. Furthermore, the error analysis of Tsao *et al.* [14] enables quantitative estimation of the systematical errors involved to be made. In realistic simulations, however, a detailed quantitative error analysis, which requires substantial computational effort, will not be necessary. Instead, one will monitor the variance and the time lags at the initial, final, and a few intermediate stages of the switching process to gain a qualitative insight into their variation during the process. Accordingly, one can choose a proper switching function to reduce the systematic and statistical errors to within a few percent.

ACKNOWLEDGMENTS

The simulations were performed on an IBM RISC/6000 computer of the CENAPAD-SP Computer Center. The authors gratefully acknowledge the financial support granted by the Brazilian funding agencies CAPES and CNPq.

APPENDIX: THE HERTZ INVARIANT

In this Appendix we review the original demonstration of the adiabatic invariance principle as presented by Hertz in 1910 [10]. We consider a system which possesses an externally controllable variable λ. We assume

the dynamics of the system is ergodic and conserves energy (not necessarily Hamiltonian) for fixed λ. In other words, for any fixed λ the dynamics propagates the state of the system (p,q) through all states of the constant energy shell $\sigma(E,\lambda)$. Furthermore, we suppose that the dynamics is deterministic, i.e., any initial condition determines a unique trajectory in phase space. The energy of the system is a function of the phase-space coordinates (p,q) and λ:

$$E = E(p,q,\lambda). \tag{A1}$$

Let us consider the constant energy shell $\sigma(E_0,\lambda_0)$ with phase-space volume Ω_0 as explored by the dynamics for the fixed value λ_0 of the parameter λ. Suppose we change λ adiabatically by an infinitesimal amount $\delta\lambda$. In what manner does the initial constant energy shell change? To answer this question we first compute the energy change δE corresponding to the adiabatic increment $\delta\lambda$. For this purpose we divide the total increment $\delta\lambda$ into a large number of smaller increments $\delta\lambda_i$ so that

$$\delta\lambda = \sum_i \delta\lambda_i. \tag{A2}$$

The increments $\delta\lambda_i$ are established in time intervals very short with respect to the ergodic time scale. On the other hand, to guarantee adiabaticity, the time intervals separating two consecutive increments λ_i are taken to be much larger than the ergodic time scale.

During a single increment $\delta\lambda_i$ the energy of a certain state (p,q) will change abruptly by an amount

$$\delta E_i = \delta\lambda_i \left.\frac{\partial E}{\partial\lambda}\right|_{E_i,\lambda_i}, \tag{A3}$$

where the derivative is calculated in the temporary state (p,q) on the temporary energy shell $\sigma(E_i,\lambda_i)$. After completing all steps the total energy change will be

$$\delta E = \sum_i \delta\lambda_i \left.\frac{\partial E}{\partial\lambda}\right|_{E_i,\lambda_i}. \tag{A4}$$

Allowing infinitely small errors of second order in the $\delta\lambda_i$ we may replace (A4) by

$$\delta E = \sum_i \delta\lambda_i \left.\frac{\partial E}{\partial\lambda}\right|_{E_0,\lambda_0}, \tag{A5}$$

calculating all derivatives on the initial constant energy shell. In principle, the total energy changes are different for all states on the initial energy shell since the derivative of the energy with respect to λ is a function of (p,q). However, recalling the fact that the time intervals between consecutive increments are very large and the fact that the dynamics is ergodic, we see that during the total increment all possible arguments (p,q) on $\sigma(E_0,\lambda_0)$ for the derivative are sampled. Thus we may write (A5) as

$$\delta E = \left\langle \left.\frac{\partial E}{\partial\lambda}\right|_{E_0,\lambda_0} \right\rangle \sum_i \delta\lambda_i = \left\langle \left.\frac{\partial E}{\partial\lambda}\right|_{E_0,\lambda_0} \right\rangle \delta\lambda, \tag{A6}$$

where $\left\langle \partial E/\partial\lambda|_{E_0,\lambda_0} \right\rangle$ is the microcanonical ensemble average of the phase function $\partial E/\partial\lambda$ over the constant energy shell $\sigma(E_0,\lambda_0)$. We see that all states (p,q) initially on the constant energy shell $\sigma(E_0,\lambda_0)$ finally lie on a new constant energy shell $\sigma(E_0+\delta E,\lambda_0+\delta\lambda)$. Since we assumed the dynamics to be deterministic this implies that the initial shell $\sigma(E_0,\lambda_0)$ is precisely mapped upon the final shell $\sigma(E_0+\delta E,\lambda_0+\delta\lambda)$.

What is the phase-space volume of the final shell? The total derivative of the phase-space volume Ω with respect to λ can be written as

$$\frac{d\Omega}{d\lambda} = \frac{\partial\Omega}{\partial\lambda} + \frac{\partial\Omega}{\partial E}\frac{\partial E}{\partial\lambda}. \tag{A7}$$

First, we evaluate $\partial\Omega/\partial\lambda$. Consider Fig. 9, where two constant energy shells $\sigma(E_0,\lambda_0)$ and $\sigma(E_0,\lambda_0+\delta\lambda)$ have been depicted. The phase-space volume difference $\delta\Omega$ between the two shells is given by

$$\begin{aligned}\delta\Omega &= \int_{\sigma(E_0,\lambda_0)} \vec{dn}\cdot\vec{d\sigma} \\ &= \int_{\sigma(E_0,\lambda_0)} \vec{dn}\cdot\frac{(\vec{\nabla}E)_{p_0,q_0,\lambda_0}}{\left|(\vec{\nabla}E)_{p_0,q_0,\lambda_0}\right|}d\sigma,\end{aligned} \tag{A8}$$

where $\vec{dn}$ is a vector perpendicular to $\sigma(E_0,\lambda_0)$, connecting its states (p_0,q_0) with their opposites (p_1,q_1) on $\sigma(E_0,\lambda_0+\delta\lambda)$. The operator $\vec{\nabla}$ represents the $2n$-dimensional phase-space gradient. In order to evaluate the dot product in (A8) we compute the energy $E(p_1,q_1,\lambda_0+\delta\lambda)$ in terms of Taylor expansions about $E(p_0,q_0,\lambda_0)$. We have

$$\begin{aligned}E(p_1,q_1,\lambda_0+\delta\lambda) = E_0 &+ \vec{dn}\cdot\left(\vec{\nabla}E\right)_{p_0,q_0,\lambda_0} \\ &+\delta\lambda\left.\frac{\partial E}{\partial\lambda}\right|_{p_0,q_0,\lambda_0} = E_0.\end{aligned} \tag{A9}$$

In this manner, we find

$$\vec{dn}\cdot\left(\vec{\nabla}E\right)_{p_0,q_0,\lambda_0} = -\delta\lambda\left.\frac{\partial E}{\partial\lambda}\right|_{p_0,q_0,\lambda_0}. \tag{A10}$$

Inserting (A10) into (A8) we find

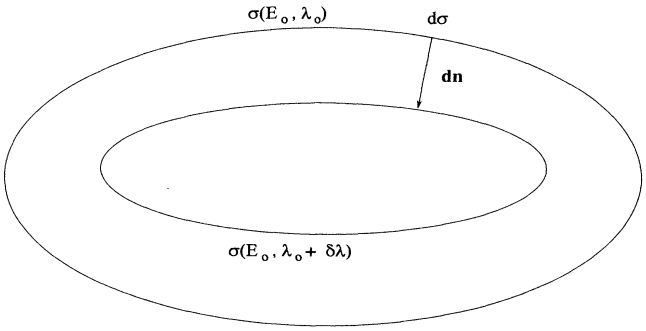

FIG. 9. The energy shells $\sigma(E_0,\lambda_0)$ and $\sigma(E_0,\lambda_0+\delta\lambda)$.

$$\left.\frac{\partial\Omega}{\partial\lambda}\right|_{E_0,\lambda_0} = -\int_{\sigma E_0,\lambda_0} \frac{d\sigma}{\left|\left(\vec{\nabla}E\right)_{p_0,q_0,\lambda_0}\right|} \left.\frac{\partial E}{\partial\lambda}\right|_{p_0,q_0,\lambda_0}. \tag{A11}$$

Apart from normalization, the surface integral in (A11) is exactly equal to the microcanonical ensemble average of the phase function $\partial E/\partial\lambda$ over the constant energy shell $\sigma(E_0,\lambda_0)$. Consequently, (A11) can be written as

$$\left.\frac{\partial\Omega}{\partial\lambda}\right|_{E_0,\lambda_0} = -\omega\left(E_0,\lambda_0\right)\left\langle \left.\frac{\partial E}{\partial\lambda}\right|_{E_0,\lambda_0}\right\rangle, \tag{A12}$$

where

$$\omega\left(E_0,\lambda_0\right) = \left.\frac{\partial\Omega}{\partial E}\right|_{E_0,\lambda_0} \tag{A13}$$

is the so-called structure function of the microcanonical ensemble and represents the normalization. Inserting (A12), (A13), and (A6) into (A7) we find

$$\left.\frac{d\Omega}{d\lambda}\right|_{E_0,\lambda_0} = 0. \tag{A14}$$

We see that the adiabatic transformation leaves the total phase-space volume unaltered.

The Hertz invariance principle implies that, in an adiabatic transformation of an ergodic deterministic energy conserving dynamics (not necessarily Hamiltonian), a constant energy shell of the initial dynamics is mapped upon a constant energy shell of the final dynamics conserving the total phase-space volume.

[1] M.P. Allen and D.J. Tildesley, *Computer Simulation of Liquids* (Oxford University Press, Oxford, 1989).

[2] *Molecular Dynamics Simulation of Statistical-Mechanical Systems*, edited by G. Ciccotti and W.G. Hoover (North-Holland, Amsterdam, 1986).

[3] *Simulation of Liquids and Solids*, edited by G. Ciccotti, D. Frenkel, and I.R. McDonald (North-Holland, Amsterdam, 1987).

[4] R. LeSar, R. Najafabadi, and D.J. Srolovitz, Phys. Rev. Lett. **63**, 624 (1989).

[5] T.H.K Barron and M.L. Klein, in *Dynamical Properties of Solids*, edited by G.K. Horton and A.A Maradudin (North-Holland, Amsterdam, 1974), Vol. 1, pp. 391–450.

[6] L. Zhao, R. Najafabadi, and D.J. Srolovitz, Modelling Simul. Mater. Sci. Eng. **1**, 539 (1993).

[7] R. Najafabadi, D.J. Srolovitz, and R. LeSar, J. Mater. Res. **5**, 2663 (1990).

[8] T.P. Straatsma, H.J.C. Berendsen, and J.P.M. Postma, J. Chem. Phys. **11**, 6720 (1986).

[9] M. Watanabe and W.P. Reinhardt, Phys. Rev. Lett. **65**, 3301 (1990).

[10] P. Hertz, Ann. Phys. (Leipzig) **33**, 537 (1910).

[11] S. Nosé, J. Chem. Phys. **81**, 511 (1984).

[12] W.G. Hoover, Phys. Rev. A **31** 1695 (1985).

[13] C. Jarzynski, Phys. Rev. A **46**, 7498 (1992).

[14] L.W. Tsao, S.Y. Sheu, and C.Y. Mou, J. Chem. Phys. **101**, 2302 (1994).

[15] G.J. Martyna, M.L. Klein, and M. Tuckerman, J. Chem. Phys. **97**, 2635 (1992).

[16] E. Smargiassi and P.A. Madden, Phys. Rev. B **51**, 117 (1995).

[17] B.L. Holian, H.A. Posch, and W.G. Hoover, Phys. Rev. E **47**, 3852 (1993).

[18] R.H. Wood, J. Phys. Chem. **95**, 4838 (1991).

[19] L. Onsager, Phys. Rev. **37**, 405 (1931); **38**, 2265 (1931).

[20] D. Kusnezov, A. Bulgac, and W. Bauer, Ann. Phys. (N.Y.) **204**, 155 (1990).

[21] I.P. Hamilton, Phys. Rev. A **42**, 7467 (1990).

[22] R.G. Winkler, Phys. Rev. A **45**, 2250 (1992).

[23] S. Toxvaerd, Phys. Rev. E **47**, 343 (1993).